Crystal structure of an oxygen-binding heme domain related to soluble guanylate cyclases

Patricia Pellicena*, David S. Karow[†], Elizabeth M. Boon[‡], Michael A. Marletta*^{‡§}, and John Kuriyan*^{‡§¶}

Departments of *Molecular and Cell Biology and [†]Chemistry, University of California, Berkeley, CA 94720; [†]Program in Cellular and Molecular Biology, University of Michigan, Ann Arbor, MI 48109; and [§]Physical Biosciences Division, Lawrence Berkeley National Laboratory, Berkeley, CA 94720

Contributed by John Kuriyan, July 16, 2004

Soluble quanylate cyclases are nitric oxide-responsive signaling proteins in which the nitric oxide sensor is a heme-binding domain of unknown structure that we have termed the heme-NO and oxygen binding (H-NOX) domain. H-NOX domains are also found in bacteria, either as isolated domains, or are fused through a membrane-spanning region to methyl-accepting chemotaxis proteins. We have determined the crystal structure of an oxygen-binding H-NOX domain of one such signaling protein from the obligate anaerobe Thermoanaerobacter tengcongensis at 1.77-Å resolution, revealing a protein fold unrelated to known structures. Particularly striking is the structure of the protoporphyrin IX group, which is distorted from planarity to an extent not seen before in proteinbound heme groups. Comparison of the structure of the H-NOX domain in two different crystal forms suggests a mechanism whereby alteration in the degree of distortion of the heme group is coupled to changes on the molecular surface of the H-NOX domain and potentially to changes in intermolecular interactions.

eme-based sensors are a diverse group of signal transduction proteins that respond to gases like nitric oxide (NO), oxygen (O₂), and carbon monoxide (CO). These proteins typically contain two distinct domains: a heme-containing sensor domain that binds to gaseous ligands, and an effector domain that generates an output signal (1, 2). There are four distinct families of heme-based sensor proteins that have been characterized. The bacterial oxygen sensors, FixL and HemAT, and the CO sensor CooA from Rhodospirillum rubrum are representative members of three of these families for which crystal structures have been determined (3–8). Whereas the proteins from these three families use the same heme cofactor (protoporphyrin IX), they have quite distinct heme-binding protein scaffolds. The oxygen sensors HemAT and FixL contain a globin fold and a PAS domain fold, respectively (3, 4, 6). The CO sensor CooA belongs to the cAMP receptor protein family of transcriptional regulators (9), and its structure is unrelated to the globin or PAS domain folds (7).

The fourth family of heme-based sensor proteins include the soluble guanylate cyclases, which are signal transduction proteins that respond to nitric oxide, a potent modulator of cardiovascular physiology in mammals (10, 11). The soluble guanylate cyclases in vertebrates, which are heterodimers of α - and β -subunits, are the only known direct sensors of NO. The heme (protoporphyrin IX)-binding domain is localized to the N terminus of the β -subunit (12, 13), and is unrelated in sequence to the heme-based sensor domains described above. Soluble guanylate cyclases bind to and become activated by picomolar amounts of NO, even in the presence of micromolar concentrations of oxygen (14, 15), and upon activation they catalyze the conversion of GTP to cGMP (15–17).

A group of prokaryotic proteins that are clearly related in sequence to the NO-binding module of soluble guanylate cyclases have been identified recently (refs. 18–20 and Fig. 1). In facultative aerobes, these domains are predicted to contain ≈ 190 residues and appear to be part of a histidine kinase operon. Homologous domains are found in obligate anaerobes, where they are fused through a membrane-spanning region to a pre-

dicted methyl-accepting chemotaxis protein domain. The heme domains from facultative aerobes that we have isolated bind NO, but not oxygen, as is the case with vertebrate soluble guanylate cyclases. In contrast, the heme domain from the methyl-accepting chemotaxis protein from *Thermoanaerobacter tengcongensis*, an obligate anaerobe, and that from the *Caenorhabditis elegans* soluble guanylate cyclase GCY-35, bind oxygen (20, 21). We refer to these domains as heme-NO and oxygen-binding (H-NOX) domains. These domains have also been named heme-NO-binding (H-NOB) domains (18), but, in light of the recently discovered specificity of some of these domains for oxygen (20), we prefer the term H-NOX.

Dysregulation of cyclase activity has been associated with several pathophysiological states, particularly those of the cardiovascular system (22). There is, as a consequence, considerable interest in obtaining structural information on these proteins, which have, however, proven to be difficult to crystallize. The crystal structure of the heterodimeric C1 and C2 catalytic domains of adenylate cyclase has been reported (23, 24), and by using the homologous regions from the α - and β -subunits of guanylate cyclase, the catalytic site of guanylate cyclase has been modeled (25). Furthermore, we have shown that reconstituted activity requires both the α and β catalytic domains (J. Winger and M.A.M., unpublished results). Whereas catalysis requires heterodimer formation, the spectral and specific ligand-binding properties of the heme domain do not. A homodimeric construct of residues 1-385 of the β -subunit has all of the spectral characteristics of the native enzyme (13, 26) as does a shorter monomeric construct of residues 1-194 (D.S.K. and M.A.M., unpublished results). No structural templates are available for the sensor heme domain.

Here, we report the crystal structure of the liganded H-NOX domain of the chemotaxis receptor from *T. tengcongensis*. The H-NOX domain is shown to have a protein fold in which a tightly packed central cavity houses an unusually distorted heme group. Comparison of the conformation of the H-NOX domain in two different space groups reveals significant differences that provide some clues to the mechanism by which the conformation of the heme may be coupled to structural changes on the surface of the protein, thereby providing a potential route for further transmission of the signal.

Methods

The H-NOX domain from *T. tengcongensis* was expressed in bacteria and purified as described (20). The purified H-NOX domain was isolated with bound oxygen. To generate the ferric form, oxidation of the heme iron was accomplished as described (20). Crystals were grown by using the hanging-drop vapor

Freely available online through the PNAS open access option.

Abbreviations: H-NOX, heme NO and oxygen binding; O_2 , oxygen.

Data deposition: The atomic coordinates have been deposited in the Protein Data Bank, www.pdb.org (PDB ID codes 1U4H, 1U55, and 1U56).

 $^{
m 1}$ To whom correspondence should be addressed. E-mail: kuriyan@berkeley.edu.

© 2004 by The National Academy of Sciences of the USA

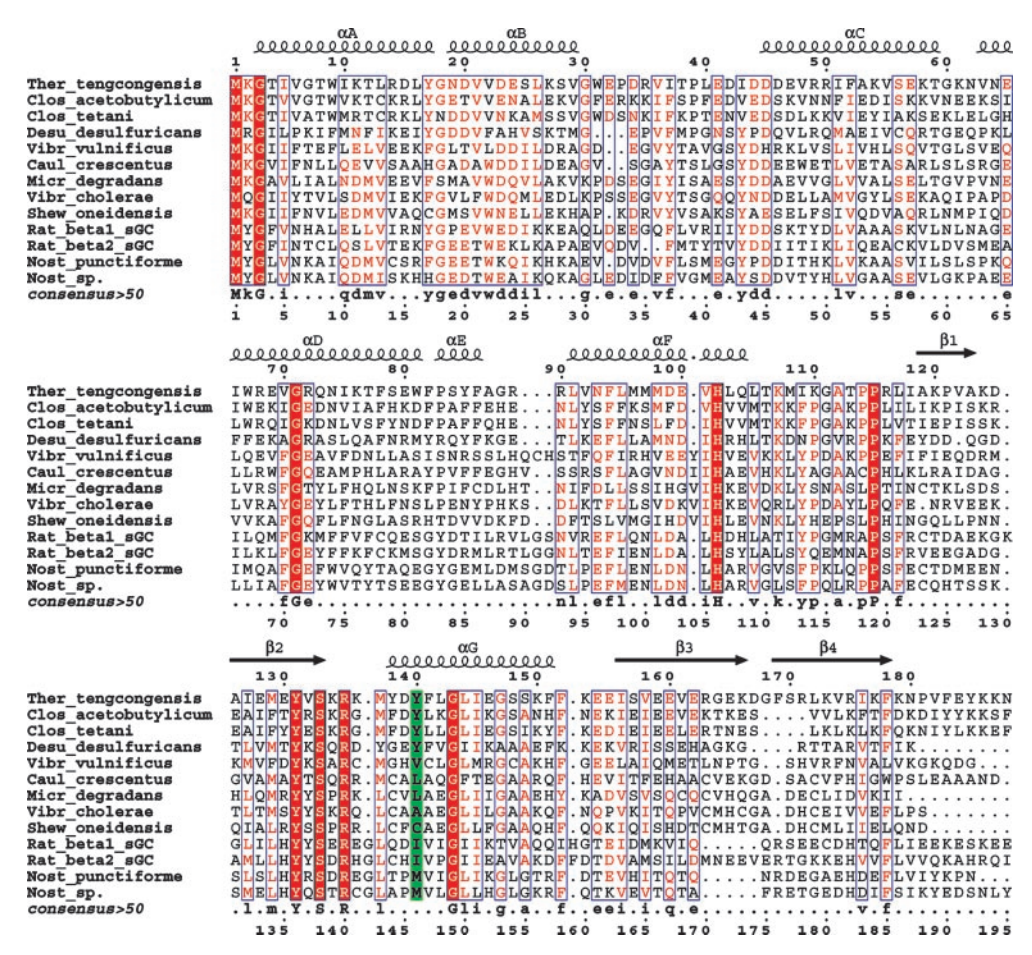


Fig. 1. Multiple sequence alignment of selected H-NOX domains. Secondary structure annotation, and numbering on top, correspond to the H-NOX domain from T. tengcongensis. α-helices are represented by spirals and β-strands by arrows. The position of Tyr-140 is indicated by a green box. Accession numbers are as follows: Ther_tengcongensis_gi|20807169|, Clos_acetobutylicum_gi|15896488|, Desu_desulfuricans_gi|23475919|, Rat_beta1_sGC_gi|27127318|, Rat_beta2_sGC_gi|21956635|, Nost_punctiforme_gi|23129606|, Nost_sp._gi|17229770|, Vibr_vulnificus_gi|27361734|, Caul_crescentus_gi|16127222|, Micr_degradans_gi|23027521|, Vibr_cholerae_gi|15601476|, and Shew_oneidensis_gi|24373702|. Alignments were carried out by using the program MULTALIN (42). Fig. 1 was prepared by using the program ESPRIPT (43).

diffusion method by mixing equal volumes of a 20 mg/ml protein solution and various crystallization solutions (generally, 0.1–0.4 M monovalent or divalent salts and 18–25% polyethylene glycol 3350), and then equilibrating over a 700- μ l reservoir of the same crystallization buffer at 20°C. Crystals appeared within 24 h. Cryoprotection was achieved by transferring the crystals stepwise into mother liquor solutions containing 5%, 10%, 15%, 20% glycerol, and ending with 20% glycerol and 5% xylitol.

We have obtained crystals of the H-NOX domain in two space groups, orthorhombic (P2₁2₁2) and monoclinic (C2), under similar conditions (see Table 2, which is published as supporting information on the PNAS web site). Crystals of selenomethionine-substituted protein only grew in the orthorhombic space group and were obtained in 0.25 M potassium thiocyanate, 20% polyethylene glycol 3350, and 10 mM DTT. Crystals of the oxygen-bound monoclinic form were grown in 0.2 M NaCl and 20% polyethylene glycol 3350. The ferric form of the protein was crystallized in 0.2 M MgCl₂, 0.1 M [bis(2-hydroxyethyl)imino]tris(hydroxymethyl)methane, pH 6.5, and 25% polyethylene glycol 3350 in the monoclinic space group. Crystals were frozen in propane and stored in liquid nitrogen for later use in data collection. All data collection was carried out at 100 K. Multiwavelength data from selenomethionine-labeled crystals (14 Se atoms per asymmetric unit) was used to obtain phase information by using the SOLVE/RESOLVE programs (27, 28). The model obtained was used subsequently to solve the structure of the protein in the monoclinic crystal forms by molecular replacement. Diffraction data were collected by using synchrotron radiation at beam lines 8.3.1 and 8.2.1 at the Advanced Light Source, Lawrence Berkeley National Laboratory. Data were integrated and reduced with the DENZO/SCALEPACK programs (29). Model building and refinement were carried out by using the programs o (30) and CNS (31). The heme was refined by using a CHARMM-based force field (32), where improper torsions that maintain planarity were removed, while restricting planarity of the pyrrole groups. The final model from the orthorhombic crystal form includes all amino acid residues (1-188) from both molecules in the asymmetric unit and 197 solvent molecules. For the monoclinic crystal form, the oxy model includes all residues for molecule A, residues 1-187 for molecule B and 269 solvent molecules. The structures of oxy (orthorhombic), oxy (monoclinic), and ferric (monoclinic) H-NOX domains were refined to 2.07-, 1.77-, and 1.90-Å resolution, respectively (Table 2).

Results and Discussion

Structure Determination. We have determined the crystal structure of the oxygen-ligated H-NOX domain (residues 1–188) of *T. tengcongensis* in the orthorhombic space group, by using multiwavelength anomalous diffraction of selenomethionine-substituted protein for experimental phase determination. We

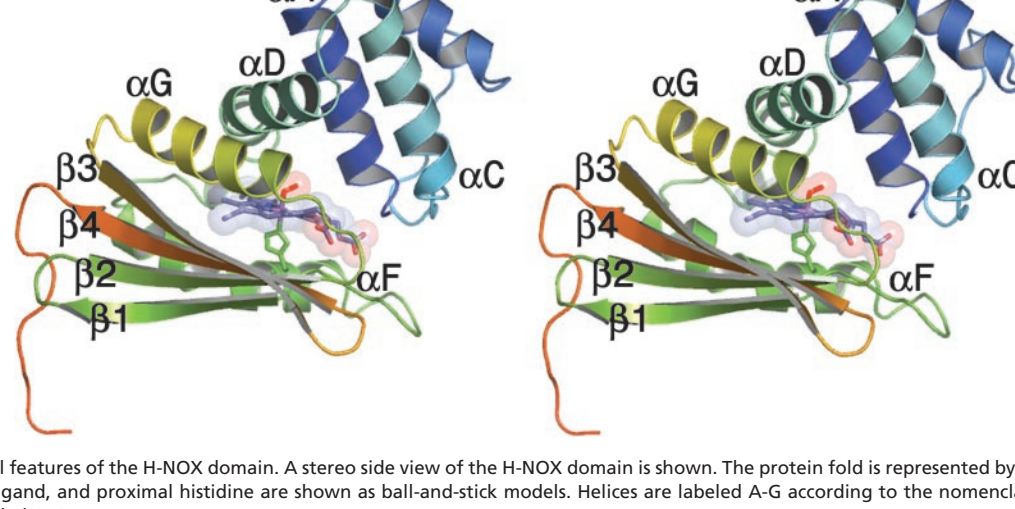


Fig. 2. Structural features of the H-NOX domain. A stereo side view of the H-NOX domain is shown. The protein fold is represented by ribbon diagrams. The heme, dioxygen ligand, and proximal histidine are shown as ball-and-stick models. Helices are labeled A-G according to the nomenclature shown in Fig. 1. β-strands are labeled 1-4.

have also solved the crystal structure of the protein in the monoclinic space group by molecular replacement in both the oxygen-bound and ferric forms. In the ferric form, there appears to be a water molecule or a hydroxide ion bound to the heme iron. Both orthorhombic and monoclinic crystal forms have two molecules per asymmetric unit.

We have not succeeded in crystallizing the unliganded form of the H-NOX domain (with a penta-coordinated iron) despite considerable effort. The H-NOX domain of T. tengcongensis has a very high affinity for its oxygen ligand (E.M.B. and M.A.M., unpublished observations) and attempts at crystallization of the reduced, deoxy H-NOX domain under anaerobic conditions have failed. Treatment of oxygen-bound or ferric crystals with the reducing agent dithionite resulted in the crystals dissolving. a decrease in resolution to \approx 7 Å, or in the incomplete conversion of one form to another, as determined by electron density maps. A mutant form of the protein with reduced affinity for oxygen (Tyr 140 Leu, E.M.B. and M.A.M., unpublished work) only crystallized once, and appeared to be oxidized. X-ray data obtained from these crystals after reduction showed evidence for a mixture of five- and six-coordinated heme groups, and could not be interpreted readily.

The Protein Fold. The H-NOX fold consists of seven α -helices, labeled α A-G, and one four-stranded antiparallel β -sheet (strands β 1–4; Fig. 2). The heme group is tightly packed within a central cavity, and is cradled on the proximal side by the β -sheet, a one-turn helix (helix αE, residues 83–86), and by helix α F (91–104), which runs parallel to the plane of the porphyrin ring. Helix αF is slightly bent and contains His-102, which is the proximal ligand to the heme iron and is invariant in all H-NOX domains (Figs. 1 and 2). The distal pocket is mainly lined by residues presented by helix αG (residues 138–151), which also runs approximately parallel to the plane of the porphyrin ring, and by helices αA and αD , which present hydrophobic residues that make contact with the heme.

A search of the protein structure database by using the program DALI (33) does not reveal significant similarity between the structure of the H-NOX domain and that of other proteins. The presence of a β -sheet in the H-NOX structure distinguishes it from the all helical globin fold. The mixture of α -helices and β -strands seen in the H-NOX domain is reminiscent of the structure of the PAS domain (34), but the fold of the H-NOX domain is unrelated to that of the PAS domain (Fig. 6, which is published as supporting information on the PNAS web site).

Heme Environment. In contrast to soluble guanylate cyclases, where spectroscopic measurements indicate that the binding of NO to the heme severs the proximal histidine-iron bond (14, 15, 35, 36), the T. Tengcongensis H-NOX domain forms a sixcoordinate NO complex (20). Other O₂-binding hemoproteins, such as the globins, also bind NO in a six-coordinate complex. Furthermore, some of the bacterial H-NOXs that do not bind O₂ bind NO in a mix of five- and six-coordinate complexes (J. Davis, D.S.K., E.M.B., and M.A.M., unpublished results) so the functional significance of ligand-induced Fe-His bond breakage remains to be established. Spectroscopic evidence shows that the H-NOX domain forms a six-coordinate ferrous oxy complex (20) and indeed, the crystal structure of the H-NOX domain shows that the iron is six-coordinate, with an iron-histidine bond distance of 2.01–2.14 Å, which is consistent with UV-visible and Raman spectroscopy studies (20). Electron density in the distal pocket is consistent with a bound dioxygen molecule, in accord with spectroscopic studies (20). Residues that line the distal pocket are exclusively nonpolar, with the exception of Tyr-140, the side chain of which forms a hydrogen bond with the oxygen ligand.

The orientation of Tyr-140 is fixed by a hydrogen bonding network involving Trp-9 and Asn-74 (Fig. 3A), which may contribute to the high affinity of the protein for oxygen. Sequence alignments of H-NOX domains (Fig. 1) reveal that a tyrosine in this position is found only in the H-NOX domains that form part of chemotaxis receptors in anaerobic organisms, and it is likely that the structural basis for ligand discrimination originates with this tyrosine residue. Residues found at this position in the H-NOX domains of facultative aerobes and in animal soluble guanylate cyclases are mostly hydrophobic (I, L, A, M, V, or C).

In the H-NOX domain, the propionate groups of the heme are buried and are tightly bound by protein side chains, a situation that contrasts with the surface exposed nature of these groups in other hemoproteins. Critical to the coordination of the propionate groups is Arg-135, which forms hydrogen bonds with both carboxyl groups and is, in turn, held in place by a series of hydrogen bonding interactions with other residues (Figs. 3B and 5). Tyr-131 and Ser-133 also coordinate one of the propionate groups, and along with Arg-135 form a "YxSxR" motif that is

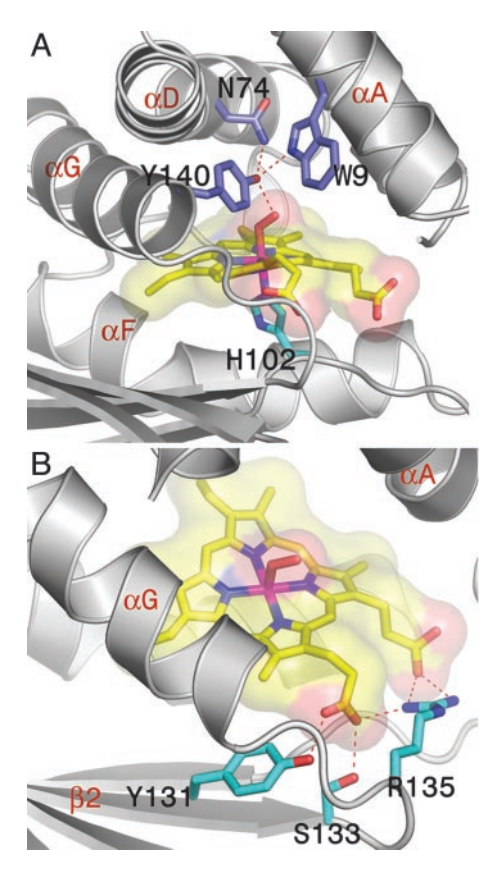


Fig. 3. Heme environment. (*A*) Ligand-binding pocket. Tyr-140 is shown hydrogen bonding (red dashes) to the heme-bound oxygen ligand. Trp-9 and Asn-74 interact with Tyr-140. The proximal ligand, His-102, is also shown. (*B*) The YxSxR motif, corresponding to residues Tyr-131, Ser-133, and Arg-135, coordinates heme propionates.

invariant in all H-NOX domains (YxTxR in *C. elegans*; Figs. 1 and 3*B*). A recent report identified Tyr-135 and Arg-139 of the YxSxR motif in human soluble guanylate cyclase as being important for heme binding (19). The N terminus of the protein is also a part of this network of interactions (Fig. 5).

Heme Distortion. The most remarkable feature of the H-NOX domain is the highly nonplanar porphyrin group (Fig. 4), the distortions of which are readily apparent in the experimentally phased electron density map (Fig. 7, which is published as supporting information on the PNAS web site). In both the ferrous-oxy and ferric structures, the iron atom is essentially coplanar with the four pyrrole nitrogen atoms, as expected for six-coordinated low-spin iron. There is, however, considerable buckling of each of the pyrrole groups with respect to the other so that the heme group as a whole is considerably distorted. Resonance Raman spectroscopy studies of the *T. tengcongensis* H-NOX domain are consistent with the presence of a distorted heme in solution (20). Whereas deviation from planarity is common in protein-bound heme groups, the extent of the distortion seen in the H-NOX domain is unprecedented among hemoproteins for which crystal structures are available.

In a reported analysis (37) of the geometry of protein-bound heme groups, it was noted that heme groups that are covalently linked to amino acid residues, such as those of the cytochromes c, are the most distorted. Among proteins with noncovalently attached hemes, peroxidases contain some of the most distorted hemes (37). Table 1 shows the rms deviation from planarity of atoms in the heme groups in the H-NOX domain structures, and compares these with values for heme groups from cytochrome c_3

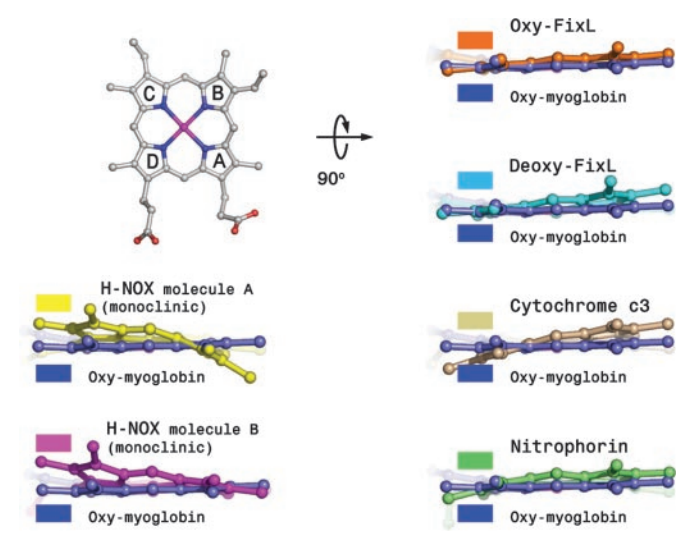


Fig. 4. Heme distortion. Schematic diagram of the heme group with pyrrole groups A–D labeled. Pyrrole groups B and C were used to superimpose the heme groups from different proteins with that of oxy-myoglobin. Heme propionates have been removed for clarity.

[2CVD (38)], a peroxidase [1ARP (39)], NO-bound nitrophorin 4 [1ERX (40)], deoxy-FixL [(1DRM (8)], oxy-FixL [(1DP6 (5)], and oxy-myoglobin [(1A6M (41)]. For 32 core atoms, excluding the propionate side chains and the iron atom, the rms deviation from planarity of the heme group in the orthorhombic H-NOX structures (\approx 0.45 Å), is greater than the values for a cytochrome c_3 (\approx 0.36 Å) and the peroxidase (\approx 0.33 Å). The distortion in the heme group of the H-NOX domain is much larger than that seen in the oxy and deoxy forms of FixL (Fig. 4), the heme sensor protein containing a PAS domain, in which changes in heme planarity have been implicated in the signaling mechanism (8).

We also analyzed heme conformations by using normal-coordinate analysis, which describes deviations from planarity in terms of low-frequency normal modes (37). Table 1 shows that the major contributions to the deformation of the H-NOX domain heme groups can be ascribed to saddling (amplitude $\approx 1 \,\text{Å}$), which involves the bending of pyrrole rings with respect

Table 1. Heme deviations from planarity

	rms deviation*	Saddling [†]	Ruffling [†]
H-NOX			
Orthorhombic			
Heme A	0.45	-1.092	-1.094
Heme B	0.44	-0.994	-1.210
Monoclinic			
Heme A	0.46	-1.069	-1.105
Heme B	0.33	-0.634	-0.814
Cytochrome c₃	0.36	1.034	-0.429
Peroxidase	0.33	-0.905	-0.660
Nitrophorin	0.26	0.356	-0.843
Deoxy-FixL	0.26	0.597	-0.375
Oxy-FixL	0.19	0.438	-0.323
Oxy-Myoglobin	0.12	0.185	0.011

RCSB protein data bank codes: Cytochrome c_3 , 2CDV heme 1 (38); peroxidase, 1ARP (39); nitrophorin, 1ERX (40); deoxy-FixL, 1DRM (8); oxy-FixL, 1DP6 (5); oxy-myoglobin, 1A6M (41).

^{*}rms deviation from planarity angstroms.

[†]Heme distortions calculated using normal-coordinate analysis (37). The numerical value shown is the displacement along the normal mode in angstroms.



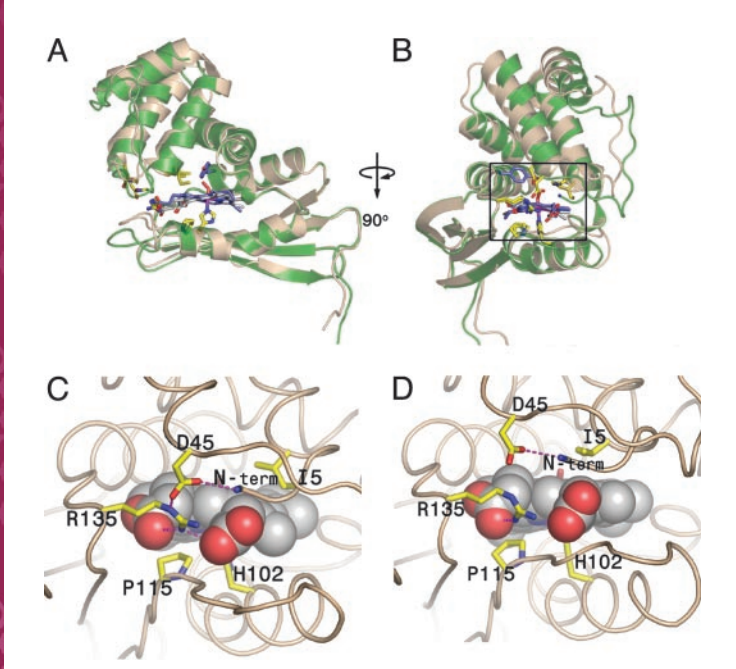


Fig. 5. Structural changes associated with different heme conformations. (A) Ribbon diagram showing the superimposition of two molecules exhibiting different heme conformations. Molecule A (monoclinic) is green and molecule B (monoclinic) is white. (B) A 90° rotation of A about the y axis. (C and D) Diagram showing the major changes in networking interactions. Molecule A (monoclinic) with the more distorted heme is shown in C. Molecule B (monoclinic), which has the less distorted heme, is shown in D. The enlargements in C and D are of the boxed area in B.

to each other, and ruffling (amplitude \approx 1.1–1.2 Å), described as a rotation of the pyrrole rings about the iron-nitrogen bonds. Notably, the combined saddling and ruffling observed in the H-NOX domain, as determined by normal-coordinate analysis, surpasses that of the peroxidases and the covalently attached hemes of the cytochromes c (Table 1). The nitrophorins are NO-binding proteins that exhibit a high degree of ligand-induced heme ruffling (40), but again, the degree to which the heme is distorted in a nitrophorin is less than that seen in the H-NOX domain.

Table 3, which is published as supporting information on the PNAS web site, lists the angles between the planes of the pyrrole groups of the heme groups in the H-NOX domain structures, and compares these structures with the corresponding angles in other proteins. The interplanar angles demonstrate the extreme distortion of the H-NOX heme groups quite strikingly. In the orthorhombic crystal form, the heme group interplanar angles range from $\approx 15^{\circ}$ to 30°. This finding contrasts with the relatively flat heme in oxy-myoglobin (interplanar angles ranging from ≈1° to $\approx 10^{\circ}$) and is significantly greater than the range of $\approx 12-20^{\circ}$ seen in cytochrome c_3 .

Structural Consequences of Conformational Relaxation in the Heme Group. The nature of ligand-induced distortions in the heme group of the H-NOX domain are unknown because we have not succeeded in crystallizing the protein in the unliganded fivecoordinated state. Nevertheless, some insight into how the geometry of the heme group may be coupled to conformational changes in the protein is provided by the monoclinic crystal form, in which molecule B has a heme group that is significantly less distorted than in the other molecules. Pyrrole group A and, to a lesser extent, pyrrole group B (Fig. 5 and Table 3), flatten from a bent conformation to one that is more aligned with the mean porphyrin plane, decreasing the degree of heme saddling and ruffling (Table 1). This relaxation in heme strain is correlated with changes in the structure of the protein that are suggestive of a mechanism that couples heme geometry to significant structural changes on the surface of the protein. These changes appear to be a consequence of differences in crystal packing interactions (see Supporting Text, which is published as supporting information on the PNAS web site) that are coupled to the heme group.

Upon comparing molecule B in the monoclinic crystal form with molecule A in the orthorhombic form, we find that the portion of the protein that is on the proximal side of the heme group superimposes very well between the A and B molecules (Fig. 5). There is, however, a significant relative rotation of the distal half of the protein with respect to the proximal half, by ≈11°, between the two molecules. The origin of this rotation can be traced to changes in the planarity of the heme group and, specifically, to a change in the conformation of Ile-5 and its orientation with respect to the heme group. The movement of Ile-5, which energy minimizations have identified as the residue most important for maintaining heme distortion (see Supporting Text, and Table 4, which are published as supporting information on the PNAS web site), is correlated with a flattening of pyrrole group A, and is tracked by the very N-terminal segment of the protein (Fig. 5). In particular, the amino group of the polypeptide chain (Met-1) maintains its hydrogen bond with Asp-45, and Asp-45 tracks the movement of Met-1 away from the heme group. In the structures with more distorted heme groups (e.g., molecule A of both orthorhombic and monoclinic crystal forms) Asp-45 is hydrogen-bonded to Arg-135, which coordinates the propionate groups of the heme. The movement of Asp-45 upon heme flattening breaks its interaction with Arg-135 (Fig. 5).

In the molecules with the more distorted heme groups, the angle between the A and D pyrrole groups ranges from ≈23° to 27°. This angle decreases to 11° in the flatter heme group in molecule B (monoclinic; Table 3). The change in interplanar angles between the pyrrole groups is transmitted to the propionate side chains that are connected to these pyrrole groups. The carboxyl groups of the propionate chains are closer together in the bent heme structures, and are further apart by ≈ 1 Å in the flatter heme structure (molecule B, monoclinic; Fig. 5).

In molecule A (orthorhombic or monoclinic), the terminal imino nitrogen group (NH1) of Arg-135 is approximately midway between the two oxygen atoms of the propionate chains, making strong hydrogen bonds to both. When the heme in molecule B relaxes and the inter-oxygen distance increases, the arginine side chain no longer makes a hydrogen bond to the propionate group that is attached to pyrrole D of the heme (Fig. 5). This movement of Arg-135 is coupled to the loss of its interaction with Asp-45, and the change in the position of Asp-45 is therefore coupled to the degree of heme planarity in two ways.

The actual nature of the conformational changes that occur upon ligand binding and release will only be known with certainty after the structure of an unliganded H-NOX domain is determined. Nevertheless, the fortuitous changes in structure that we have observed here are likely to be indicative of the general signaling mechanism because of the strong conservation across evolution of the elements that are involved in coupling the structural changes to the degree of heme planarity. Ile-5 is conserved as Ile, Val, or Leu, and its location five residues from the N terminus is also conserved. Although valine is a less bulky side chain, the critical interaction between Ile-5 and pyrrole group A is made by the Cy1 atom of the branched isoleucine side chain, an interaction that would be preserved in valine. The turn structure that connects Ile-5 to the N terminus is also likely to be conserved because of the presence of an invariant glycine at position 3 (Fig. 1). Asp-45 is highly conserved, as is Arg-135 (which is part of the invariant YxSxR motif). Leu-144 and

Pro-115, important for maintenance of the heme distortion, are also highly conserved.

Concluding Remarks

Structure-function studies on soluble guanylate cyclases have been hampered by the lack of structural information on the heme-binding sensor domain. The recent explosion of microbial genomic data has allowed the discovery of related domains in prokaryotes (18–20), leading to the definition of the H-NOX domain. The structure of the H-NOX domain presented here reveals a heme-binding scaffold that is conserved among prokaryotic H-NOX domains and animal soluble guanylate cyclases, as indicated by sequence alignments. A recent study (21) has shown an oxygen-dependent behavioral response in C. elegans linked to the predicted soluble guanylate cyclase gene GCY-35. The H-NOX domain of GCY-35 is the first of the soluble guanylate cyclase family to bind oxygen, strengthening the significance of the work presented here as a good foundation for understanding soluble guanylate cyclase function. The sequence alignments also suggest that the determinants of the highly distorted heme geometry seen in the T. tengcongensis H-NOX

- 1. Chan, M. K. (2001) Curr. Opin. Chem. Biol. 5, 216-222.
- 2. Rodgers, K. R. (1999) Curr. Opin. Chem. Biol. 3, 158-167.
- Gong, W., Hao, B., Mansy, S. S., Gonzalez, G., Gilles-Gonzalez, M. A. & Chan, M. K. (1998) Proc. Natl. Acad. Sci. USA 95, 15177–15182.
- 4. Zhang, W. & Phillips, G. N., Jr. (2003) Structure (London) 11, 1097-1110.
- 5. Gong, W., Hao, B. & Chan, M. K. (2000) Biochemistry 39, 3955-3962.
- Miyatake, H., Mukai, M., Park, S. Y., Adachi, S., Tamura, K., Nakamura, H., Nakamura, K., Tsuchiya, T., Iizuka, T. & Shiro, Y. (2000) J. Mol. Biol. 301, 415–431.
- Lanzilotta, W. N., Schuller, D. J., Thorsteinsson, M. V., Kerby, R. L., Roberts, G. P. & Poulos, T. L. (2000) Nat. Struct. Biol. 7, 876–880.
- Hao, B., Isaza, C., Arndt, J., Soltis, M. & Chan, M. K. (2002) Biochemistry 41, 12952–12958.
- Shelver, D., Kerby, R. L., He, Y. & Roberts, G. P. (1997) Proc. Natl. Acad. Sci. USA 94, 11216–11220.
- 10. Moncada, S., Palmer, R. M. & Higgs, E. A. (1991) *Pharmacol. Rev.* 43, 109–142.
- Denninger, J. W. & Marletta, M. A. (1999) Biochim. Biophys. Acta 1411, 334–350.
- Wedel, B., Humbert, P., Harteneck, C., Foerster, J., Malkewitz, J., Bohme, E., Schultz, G. & Koesling, D. (1994) Proc. Natl. Acad. Sci. USA 91, 2592–2596.
- Zhao, Y., Schelvis, J. P., Babcock, G. T. & Marletta, M. A. (1998) *Biochemistry* 37, 4502–4509.
- 14. Gerzer, R., Hofmann, F. & Schultz, G. (1981) Eur. J. Biochem. 116, 479-486.
- 15. Stone, J. R. & Marletta, M. A. (1994) Biochemistry 33, 5636-5640.
- Ignarro, L. J., Wood, K. S. & Wolin, M. S. (1982) Proc. Natl. Acad. Sci. USA 79, 2870–2873.
- 17. Wolin, M. S., Wood, K. S. & Ignarro, L. J. (1982) J. Biol. Chem. 257, 13312-13320.
- 18. Iyer, L. M., Anantharaman, V. & Aravind, L. (2003) BMC Genomics 4, 5.
- Schmidt, P. M., Schramm, M., Schroder, H., Wunder, F. & Stasch, J. P. (2004)
 J. Biol. Chem. 279, 3025–3032.
- Karow, D. S., Pan, D., Pellicena, P., Presley, A., Mathies, R. A. & Marletta, M. A. (2004) *Biochemistry* 43, 10203–10211.
- Gray, J. M., Karow, D. S., Lu, H., Chang, A. J., Chang, J. S., Ellis, R. E., Marletta, M. A. & Bargmann, C. I. (2004) *Nature* 430, 317–322.
- 22. Hobbs, A. J. (2002) Br. J. Pharmacol. **136**, 637–640.

domain are highly conserved, suggesting that changes in heme distortion may be an important component of the signaling mechanism of these domains. It is difficult to speculate about the nature of the unliganded state, but the structural comparisons we have presented here between different crystal forms of the liganded state provide a potential mechanism for coupling between heme flattening and substantial changes in the structure of the H-NOX domain. Just how such changes are further transmitted to downstream events will be a major focus for future study.

We thank M. Roshni Ray for technical assistance; Lore Leighton for assistance with the illustrations; and Bhushan Nagar, Greg Bowman, Holger Sondermann, Xuewu Zhang, and James Holton for assistance and advice during the process of data collection and refinement. This work was supported in part by the Laboratory Directed Research and Development Fund of the Lawrence Berkeley National Laboratory. P.P. and E.M.B. are supported by Ruth L. Kirschstein National Research Service awards. The Advanced Light Source is supported by the U.S. Department of Energy under Contract DE-AC03-76SF00098 at the Lawrence Berkeley National Laboratory.

- Zhang, G., Liu, Y., Ruoho, A. E. & Hurley, J. H. (1997) Nature 386, 247– 253
- Tesmer, J. J., Sunahara, R. K., Johnson, R. A., Gosselin, G., Gilman, A. G. & Sprang, S. R. (1999) Science 285, 756–760.
- Liu, Y., Ruoho, A. E., Rao, V. D. & Hurley, J. H. (1997) Proc. Natl. Acad. Sci. USA 94, 13414–13419.
- 26. Zhao, Y. & Marletta, M. A. (1997) Biochemistry 36, 15959-15964.
- 27. Terwilliger, T. C. & Berendzen, J. (1999) Acta Crystallogr. D 55, 849-861.
- 28. Terwilliger, T. C. & Berendzen, J. (1999) Acta Crystallogr. D 55, 501-505.
- 29. Otwinowski, Z. & Minor, W. (1997) Methods Enzymol. 276, 307–326.
- Jones, T. A., Zou, J. Y., Cowan, S. W. & Kjeldgaard. (1991) Acta Crystallogr. A 47, 110–119.
- Brunger, A. T., Adams, P. D., Clore, G. M., DeLano, W. L., Gros, P., Grosse-Kunstleve, R. W., Jiang, J. S., Kuszewski, J., Nilges, M., Pannu, N. S., et al. (1998) Acta Crystallogr. D 54, 905–921.
- 32. Kuczera, K., Kuriyan, J. & Karplus, M. (1990) J. Mol. Biol. 213, 351-373.
- 33. Holm, L. & Sander, C. (1993) *J. Mol. Biol.* **233**, 123–138.
- Borgstahl, G. E., Williams, D. R. & Getzoff, E. D. (1995) Biochemistry 34, 6278–6287.
- Makino, R., Matsuda, H., Obayashi, E., Shiro, Y., Iizuka, T. & Hori, H. (1999)
 J. Biol. Chem. 274, 7714-7723.
- Zhao, Y., Brandish, P. E., Ballou, D. P. & Marletta, M. A. (1999) Proc. Natl. Acad. Sci. USA 96, 14753–14758.
- 37. Jentzen, W., Ma, J. G. & Shelnutt, J. A. (1998) Biophys. J. 74, 753-763.
- Higuchi, Y., Kusunoki, M., Matsuura, Y., Yasuoka, N. & Kakudo, M. (1984)
 J. Mol. Biol. 172, 109–139.
- Kunishima, N., Fukuyama, K., Matsubara, H., Hatanaka, H., Shibano, Y. & Amachi, T. (1994) J. Mol. Biol. 235, 331–344.
- Roberts, S. A., Weichsel, A., Qiu, Y., Shelnutt, J. A., Walker, F. A. & Montfort, W. R. (2001) *Biochemistry* 40, 11327–11337.
- Vojtechovsky, J., Chu, K., Berendzen, J., Sweet, R. M. & Schlichting, I. (1999) Biophys. J. 77, 2153–2174.
- 42. Corpet, F. (1988) Nucleic Acids Res. 16, 10881-10890.
- Gouet, P., Courcelle, E., Stuart, D. I. & Metoz, F. (1999) Bioinformatics 15, 305–308.